Carbohydrate Polymers 132 (2015) 520–528

Contents lists available at ScienceDirect

Carbohydrate Polymers

journal homepage: www.elsevier.com/locate/carbpol

Photo-responsive shell cross-linked micelles based on carboxymethyl chitosan and their application in controlled release of pesticide

Zhao Ye, Jingjing Guo, Dewei Wu, Mingyuan Tan, Xiong Xiong, Yihua Yin*, Guanghua He*

Department of Pharmaceutical Engineering, School of Chemistry, Chemical Engineering and Life Science, Wuhan University of Technology, Wuhan 430070, PR China

ARTICLE INFO

Article history:
Received 21 March 2015
Received in revised form 16 June 2015
Accepted 17 June 2015
Available online 2 July 2015

Keywords:
Carboxymethyl chitosan
Core–shell micelles
Photo-responsibility
Pesticide delivery

ABSTRACT

An amphiphilic carboxymethyl chitosan conjugate with photolabile 2-nitrobenzyl side groups (NBS–CMCS) was synthesized, which could self-assemble into polymeric micelles in aqueous condition following by adding dropwise dialdehyde to form a cross-linking structure. TEM and ^{1}H NMR confirmed that the cross-linked micelles had a core–shell configuration with an average diameter of 140 ± 5.5 nm. DLS and TEM observations showed that the cross-linked micelles were stable in aqueous solution at pH 7.0 without light irradiation, while they could transfer into nanocapsules upon exposure to 365 nm UV light. Diuron, a photosynthetic inhibitor, was encapsulated in the cross-linked micelles reaching encapsulation efficiency as much as 91.9%. No release of the encapsulated diuron was detected without light, whereas a release rate as high as 96.8% over 8 h at pH 7.0 buffer was observed under solar stimulated irradiation, indicating that the cross-linked micelles may be used as a photo-controlled sustained release carrier for the delivery of photosynthetic inhibitor.

1. Introduction

The wide use of pesticide in agriculture contributes to achieving global food security but brings undesirable effects to humans and the natural environment. As much as 90% of the applied conventional pesticides never reach their objects to produce desired biological response at the precise time and in precise quantities required, due to nonspecific and periodic application of active agents. This not only increases the cost but also leads to environmental pollution (Margni, Rossier, Crettaz, & Jolliet, 2002; Yi et al., 2011). Because of the cost and other limitations in the synthesis of new pesticides, increasing attention is being paid to the development of controlled delivery systems of the pesticides (Sun et al., 2014; Tasmin et al., 2014; Yi et al., 2011). Controlled delivery technology offers the opportunity to develop formulations which can improve the performance of pesticides by increasing their efficacy and safety and making them environmentally less harmful.

Polymeric micelles (PMs) have been increasingly investigated as promising controlled delivery carriers for bioactive substances (Li et al., 2012; Mathot, van Beijsterveldt, Preat, Brewster, & Arien, 2006; Feng et al., 2013) because their hydrophobic core can serve as a reservoir for various hydrophobic bioactive agents; whereas the outer shell consisting of hydrophilic block of polymer confers aqueous solubility and steric stability, avoiding the inactivation of loaded bioactive molecules in delivery process. Importantly, PMs can resist the dilution in environmental fluid due to lower critical micelle concentration (CMC) as compared to surfactant-based micelles. Recently, PMs with photoresponsive property have gained considerable interest (Jiang, Tong, Morris, & Zhao, 2006), because of their ability to exert spatial and temporal control over the release of active substance in respond to external light stimuli. Generally, the construction of photoresponsive PMs need use a phototrigger such as coumarin, 2-nitrobenzyl, 7-nitroindoline (He, Tong, & Zhao, 2009; Jiang, Qi, Lepage, & Zhao, 2007; Wang, Ma, Wang, & Zhang, 2007) or their derivatives. Among them, 2-nitrobenzyl has attracted particular attention since it can undergo a photolysis reaction under UV light or near-infrared light (NIR), breaking the hydrophilic–hydrophobic balance of the 2-nitrobenzyl-containing polymer and leading to the disruption of PMs. For example, the micelle system based on an amphiphilic chitosan conjugate containing 2-nitrobenzyl groups was successfully synthesized by assembly technique, which could release hydrophobic anticancer drug camptothecin in response to UV-light and showed a better cytotoxicity against MCF-7 cancer cells (Meng et al., 2013). So far,

* Corresponding authors. Tel.: +86 027 87859300; fax: +86 027 87859300.
E-mail addresses: yihuayin@aliyun.com (Y. Yin), guanghuahe@126.com (G. He).

http://dx.doi.org/10.1016/j.carbpol.2015.06.077
0144-8617/

however, the photo-responsive PMs or nanospheres reported in the literature are mostly used as a carrier for controlled release of drugs, and the designs for encapsulation of pesticides for controlling release have not been reported.

Herbicides are a group of pesticides that control or eliminate the growth of weeds. Herbicides account for more than 40% of the pesticides consumed globally each year, and are the most important and broadly used agrochemicals in rice culture systems (Yamamoto & Nakamura, 2003). Herbicides have many different modes of action, one of which is inhibiting photosynthesis, a process vital to weed survival (Sopeña, Maqueda, & Morillo, 2009). When the process is disrupted for any reason, the weeds will die. Photosynthesis, therefore, is the target of a group of herbicides known as photosynthetic inhibitors. Photosynthesis requires light energy from the sun. When weeds are exposed to sunlight if a photo-controlled delivery system arrived at the target can release photosynthetic inhibitor, photosynthesis will be inhibited.

In this work, we attempted to synthesize a novel amphiphilic carboxymethyl chitosan conjugate (NBS–CMCS) by side-chain grafting of hydrophobic photosensitive 2-nitrobenzyl succinate (NBS) to the main chains of CMCS, and then using the conjugate to develop a photo-responsive shell cross-linked nanocarrier for delivery and controlled-release of photosynthetic inhibitor or herbicide. Diuron is chosen as a hydrophobic photosynthetic inhibitor which is encapsulated in the nanocarrier. The encapsulation stability and photo-triggered release behavior were evaluated. It was expected that this preparation did not release the encapsulated diruon or only a little amount was released without light irradiation, while it could release out the inhibitor to inhibit the photosynthesis of weeds once exposed to sunlight.

2. Materials and methods

2.1. Materials

Chitosan (CS, Mw = 5.6×10^5 Da) (99%) with a deacetylation degree of 91.13% was purchased from the Zhejiang Yuhuan Biotechnology Company. Succinic anhydride, *O*-nitrobenzyl alcohol, 4-(dimethylamino) pyridine (DMAP), *N*-hydroxysuccinimide (NHS), glutaraldehyde (GA) (25% in water), and Nile red were purchased from Acros Organics and used without further purification. 1-Ethyl-3-(3-(dimethylamino) propyl) carbodiimide hydrochloride (EDC) (≥99%) was obtained from Titan Chemical Corp. Dialysis tube (MWCO, 14 and 3.5 kDa) was obtained from Shanghai Lvniao Technology Corp. All the other chemicals were purchased as analytical-reagent grade from Sinopharm Chemical Reagent Corp., and used as received.

2.2. Synthesis of carboxymethyl chitosan (CMCS)

CMCS was synthesized according to the literature (Yin, Lv, Tu, Xu, & Zheng, 2010). In briefly, 10 g of chitosan was stirred with isopropanol (100 mL) for 6 h and then filtered. NaOH solution (50%, wt%) was added to the beaker with the filter residue, and this solution was fully stirred to mix evenly and then was frozen overnight. Chloroacetic acid (28.0 g, 0.29 mol) dissolved in isopropanol (30.0 mL) was then dropped onto the frozen chitosan mixture, and the mixture was stirred at a low temperature (10 °C) for 20 h. This solution was then filtered and the filter residue was washed with absolute ethanol. The crude product was then removed by centrifugation and subsequent dialysis against deionized water, and then freeze–dried to obtain CMCS. The degree of substitution (DS) of carboxymethyl groups was determined by potentiometric titration (Muzzarelli, Tanfani, Emanuel, & Mariotti, 1982). Briefly, CMCS (0.3 g) dissolved in HCl (50 mL, 0.1 mol/L) was titrated by NaOH solution (0.1 mol/L). The amount of base at the inflection point was calculated by second-order derivative method. The DS of carboxymethyl groups was obtained according to the formula: DS = Mcts $[(V_2-V_1)\ C_{NaOH}/m]/[1-58\ (V_2-V_1)\ C_{NaOH}/m]$, m is the mass of titrated carboxymethyl chitosan. Mcts is the molar mass of the glucosamine units; V_1 is the titration end of excess hydrochloric acid; V_2 is the titration end of carboxyl. The obtained total DS of carboxymethyl groups was about 0.75. The substitution degree of *N*-carboxymethyl group was about 0.22. The viscosity-average molecular weight (Mη) of CMCS was calculated according to classic Mark–Houwink equation $[\eta] = 7.92 \times 10^{-5} \times M\eta^{1.0}$ (Luo, Teng, Wang, & Wang, 2013) by measuring the intrinsic viscosity [η] of CMCS aqueous solution using an ubbelohde viscometer, its value was 5.15×10^5 Da.

2.3. Synthesis of 2-nitrobenzyl succinate (NBS)

Typically, 2-nitrobenzyl alcohol (3.83 g, 25.0 mmol), succinic anhydride (5.03 g, 50.0 mmol), and DMAP (1.53 g, 12.5 mmol) were dissolved completely in $CHCl_3$ (86 mL). The reaction mixture was refluxed overnight (24 h) under a nitrogen atmosphere. $CHCl_3$ was evaporated under reduced pressure. The mixture was washed three times with 10% HCl and then extracted with saturated $NaHCO_3$ solution. The basic aqueous phase was washed with diethyl ether and acidified to pH 5.0 with 10% HCl. The white solid precipitate was collected and dried in vacuo at 40 °C overnight to provide the product (NBS) (5.63 g, 89%). All above reactions were in dark place.

2.4. Synthesis of 2-nitrobenzyl succinate-carboxymethyl chitosan (NBS–CMCS)

NBS–CMCS was synthesized by grafting NBS onto the main chain of CMCS according to the method in literature (Kindermann, George, Johnsson, & Johnsson, 2003). In briefly, CMCS (110 mg) was dissolved completely in 15 mL deionized water. NBS (25.8 mg, 0.1 mmol), EDC (28.8 mg, 0.15 mmol), and NHS (17.3 mg, 0.15 mmol) were added into DMSO (3.0 mL) in sequence, and the reaction mixture was stirred at ambient temperature for 6 h. After that, the reaction mixture was dropwise added into the CMCS solution, and the final reaction mixture was stirred at ambient temperature for 24 h. The resulting mixture was dialyzed in deionized water for two days and followed by lyophilization to produce NBS–CMCS. The product was characterized by ^{1}H NMR spectroscopy and FT-IR spectroscopy.

In the various feed molar ratios of amino groups of CMCS and carboxyl groups of NBS, three samples were synthesized using the same method and named as NBS–CMCS-1, NBS–CMCS-2, and NBS–CMCS-3, respectively. The DS of NBS was determined by measuring the concentration of unreacted NBS in the reaction mixture through UV absorbance at 260 nm and calculated according to the equation: $DS = (M_{total} - M_{unreacted})/M_{glucosamine}$. Where M_{total}, $M_{unreacted}$, and $M_{glucosamine}$ are the amount (in moles) of NBS in feed, NBS unreacted in reaction mixture, and glucosamine unit in CMCS (Meng et al., 2013). The equation for calibration curve is $A = 0.0093C + 0.0008$, $R^2 = 0.9981$, A is the absorbance of NBS at 260 nm UV light, C is the concentration of the NBS. The DS of NBS on CMCS in three samples were 0.035, 0.066 and 0.081, respectively.

2.5. Preparation of micelles

NBS–CMCS (10.0 mg) was dissolved completely in 10 mL deionized water and pH value of the solution was adjusted to pH 7.0 under mild stirring, followed by sonication for 3 min using a probe type sonifier (JY92-2D, made by Ningbo Xinzhi Bio-tech Co., Ltd.) at 100 W using a pulse function (pulse on 2.0 s, pulse off 2.0 s), the micelle solution was obtained. The solution was filtrated through

Table 1
The mean diameters and distributions of uncross-linked micelles and cross-linked micelles based on NBS–CMCS.

Conjugates	Uncross-linked micelles			Cross-linked micelles		
	Particle diameter (nm)	Polydispersity index	Zeta potential (mV)	Particle diameter (nm)	Polydispersity index	Zeta potential (mV)
NBS–CMCS-1	242 ± 0.04	0.097 ± 0.012	−29.2 ± 1.42	217 ± 0.02	0.082 ± 0.008	−29.6 ± 1.11
NBS–CMCS-2	226 ± 0.15	0.104 ± 0.016	−25.5 ± 1.24	196 ± 0.11	0.074 ± 0.012	−26.2 ± 1.03
NBS–CMCS-1[a]	253 ± 0.12	0.114 ± 0.010	−28.2 ± 1.30	220 ± 0.03	0.072 ± 0.010	−29.4 ± 1.01
NBS–CMCS-2[b]	40.6 ± 5.13	6.136 ± 0.012	−30.5 ± 1.11	238 ± 0.20	0.065 ± 0.014	−29.2 ± 1.12

[a] The data from the NBS–CMCS-1 micelles stored for one month in the dark at pH 7.0.
[b] The data from the NBS–CMCS-2 micelles exposed to UV radiation for 10 min at pH 7.0.

0.45 μm Millipore filter and the filtrate was divided into two parts. One part was directly used for the preparation of shell cross-linked micelles, the other was dialyzed against pH 7.0 solution, and then used for analysis and testing. All operations were carried out at the dark environment.

The preparation of shell cross-linked micelles was carried out as follows: 1 mL of GA aqueous solution (1.35×10^{-2} mmol/mL) was added dropwise into the above micelle solution over 4 h under vigorous stirring at 25 °C. The resulting mixture was kept stirring for another 6 h and then further purified by dialysis (MWCO 3500 Da) in PBS solution for 24 h, and used for analysis and testing.

The degree of crosslinking (DC) of GA was estimated by measuring the concentration of unreacted GA in the reaction mixture through UV absorbance at 280 nm assuming that no intramolecular crosslinkings are formed: DC (%) = [(total GA − unreacted GA)/$M_{glucosamine}$] × 100%. where total GA, unreacted GA, and $M_{glucosamine}$ are the amount (in moles) of GA in feed, GA unreacted in reaction mixture, and glucosamine unit in CMCS.

The cross-linked micelles were prepared from NBS–CMCS-1, NBS–CMCS-2 and NBS–CMCS-3. Their DC was 18.2, 14.5 and 9.6, respectively.

2.6. Characterization of the micelles

The critical micelle concentration (CMC) of amphiphilic NBS–CMCS in aqueous media was determined by fluorescence probe technique using Nile red as a hydrphobic probe. A series of NBS–CMCS-1, NBS–CMCS-2 and NBS–CMCS-3 solutions containing 1×10^{-6} M Nile red were prepared, of which concentration varied from 5.0×10^{-3} to 0.4 mg/mL. The excitation wavelength (λex) of Nile red was 550 nm.

The average particle size and size distribution of all the micelle samples (cross-linked and uncross-linked samples) were determined by dynamic light scattering (DLS) with a Zetasizer (Malvern Instruments, Herrenberg, Germany). The measurement was carried out at a detector angle of 90°, a wavelength of 512 nm and temperature of 25 °C. Morphological evaluation of all the particles was performed by TEM using a Tecnai G220 (FEI, America).

2.7. Photoresponse of the micelles

The photoresponse of the micelles was monitored by DLS and TEM measurement. Typically, 10.0 mL of aqueous solution of uncross-linked or cross-linked micelle sample was incubated at 25 °C for 5 h and then divided into two equal parts. One part was irradiated with UV light (365 nm, 150 mW cm^{-2}) for 10 min, the other part was used as a control and kept in the dark. After that, the size and morphology of samples were determined by DLS and TEM measurement.

2.8. Preparation of diuron-loaded micelles

NBS–CMCS (100 mg) were dissolved in 100 mL deionized water in a sealed flask. The pH of solution obtained was adjusted to 7.0. Diuron dissolved in 50% aqueous acetone was added dropwise into the solution and stirred for 10 h. Then the whole solution was transferred into a dialysis bag and dialyzed against deionized water for 12 h. Water was changed once every 2 h after 4 h. The dialyzed aqueous solution was collected for diuron content determination in uncross-linked micelles.

Using the same method as in Section 2.5, the diuron-loaded cross-linked micelles was prepared by adding dropwise of GA aqueous solution (1.35×10^{-2} mmol/mL) to the above diuron-loaded uncross-linked micelle solution, and then used for diuron content determination.

To determine diuron loading efficiency (LE) and encapsulation efficiency (EE), 10 mL of diuron-loaded micelles dispersion was centrifugated at high speed of 10,000 rpm for 20 min, washed three times with a little bit of deionized water to remove the free diuron. The resultant precipitate was freeze–dried for release study. The concentrations of diuron in the decanted aqueous solution and three washing solutions were determined by HPLC using a C18 bonded reverse phase column with a mobile phase of acetonitrile-water mix (80:20, v/v), at a flow rate of 1.0 mL/min. The peak was detected at 250 nm with a UV detector. The LE and EE were calculated as follows:

$$LE(\%) = \left(\frac{W}{W_0}\right) \times 100\% \quad (1)$$

$$EE(\%) = \left(\frac{A-B}{A}\right) \times 100\% \quad (2)$$

In Eq. (1), W is the mass of drug in micelles and W_0 is the mass of drug-loaded micelles. In Eq. (2), A is the total amount of the diuron, and B is the amount of diuron remaining in the supernatant.

The LE and EE of diuron-loaded uncross-linked samples and cross-linked samples based on NBS–CMCS were determined, and their values were listed in Table 2.

2.9. Controlled-release of the diuron-loaded micelles

Lyophilized diuron-loaded uncross-linked or cross-linked micelle sample (10.0 mg) was dispersed in 4.0 mL of phosphate buffer solution (PBS) (0.1 M, pH 7.0). The resulting solution was placed into dialysis bag (cutoff molecular weight: 14,000), then the dialysis bag was introduced into vial containing 80 mL of PBS (the same as the solution in the dialysis bag). The system was exposed to UV light (365 nm, 150 mW cm^2) under stirring at 25 °C. At appropriate time intervals, 2 mL samples of solution were withdrawn from the vials and replaced by 2 mL of fresh PBS. The drug release was assayed by HPLC. The samples without UV light irradiation were also used as a control.

By solar-simulated radiation, the release of diuron-loaded micelle samples was also carried out according to the above method. The used solar simulator is a 300 W Xenon arc lamp (200–2500 nm spectral output, 50 W radiant output).

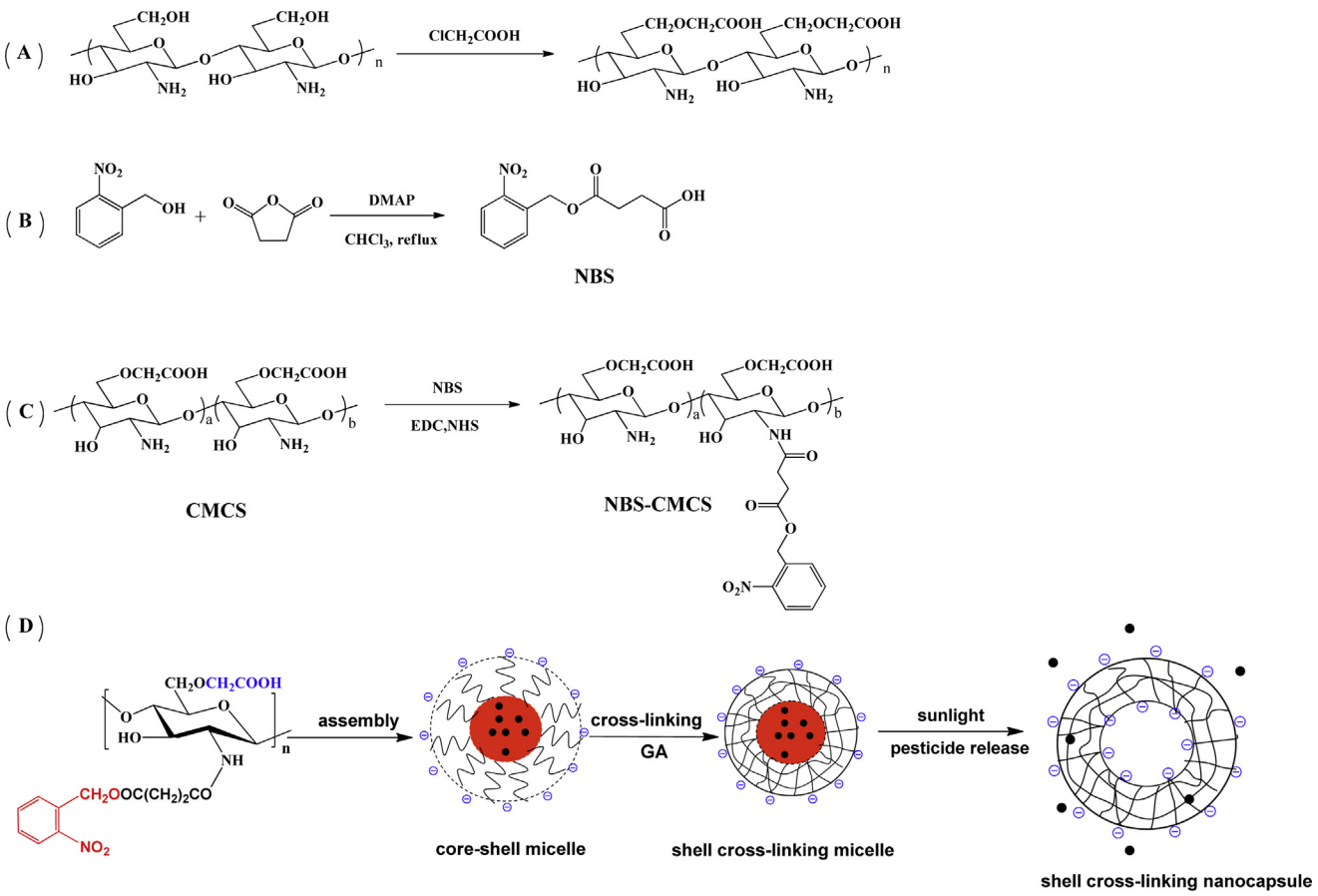

Fig. 1. Schematic illustration for the synthesis routes of (A) CMCS, (B) NBS, (C) NBS–CMCS and (D) the assembly process of NBS–CMCS.

3. Results and discussion

3.1. Synthesis and characterization of NBS–CMCS

NBS–CMCS was synthesized according to the procedure as shown in Fig. 1(A–C). During the process, 2-nitrobenzyl succinate (NBS) was firstly prepared by the esterification reaction of 2-nitrobenzyl alcohol with succinic anhydride under the catalysis of DMAP according to the literature (Meng et al., 2013; Yan, Chen, Tang, & Wang, 2004). Then, CMCS was also synthesized by the modification of chitosan with $ClCH_2COOH$ in alkaline environment. Finally, NBS was grafted onto the primary amino groups of CMCS in the presence of EDC and NHS to form NBS–CMCS. Because of the markedly different water solubility of NBS and CMCS, a mixed solvent of DMSO/deionized water (1:5, v/v) was used in the process of grafting reaction. The carboxyl acid group of NBS was first activated by NHS and then reacted with the primary amino groups in CMCS to form an amide linkage.

The ^1H NMR spectra of NBS in $CDCl_3$ and CMCS in D_2O are showed in Fig. 2. Their proton signals are assigned, respectively, as follows (ppm): for NBS (see curve a), 8.12 (d, 1H, ArH), 7.27–7.67 (m, 3H, ArH), 5.56 (s, 2H, $ArCH_2$), 2.75 (s, 4H, CH_2CH_2), which are identical with those reported in the previous papers (Meng et al., 2013; Yan et al., 2004); for CMCS, 2.107 ($COCH_3$), 3.23 (H2), 3.3–3.9 (H3, H4, H5, H6), 4.460 (H1), 4.524 (-O-CH_2-COOD), which are in accordance with the results reported before (Hjerde, Varum, Grasdalen, Tokura, & Smidsrod, 1997; Chen & Park, 2003).

The ^1H NMR spectrum of NBS–CMCS in DMSO–d_6/D_2O (1:3, v/v) is shown in Fig. 2(c). Compared with curve *b*, the appearance of new signals in the region of 7.4–8.0 ppm in curve c was the evidence of benzene ring of NBS. Those at 5.4 ppm and 2.46 ppm correspond to the benzyl methylene protons (2H, CH_2) and the succinic methylene protons (4H, CH_2CH_2), respectively. The results indicate that NBS–CMCS have been successfully synthesized.

The chemical structures of CS, CMCS and NBS–CMCS were also determined by FT-IR spectroscopy. Fig. 3 shows their results, respectively. Curve a shows the basic characteristics of chitosan at 3455 cm^{-1} (O—H stretch), 2867 cm^{-1} (C—H stretch), 1598 cm^{-1} (N—H bend), 1154 cm^{-1} (bridge-O-stretch), and 1094 cm^{-1} (C—O stretch) (Brugnerotto et al., 2001). Compared with CS (see curve a), curve b presented new characteristic bands at 1620 cm^{-1} and 1411 cm^{-1}, which were assigned to $-COO^-$ antisymmetric and symmetric stretch. The other characteristic bands of COOH should be at 3100 cm^{-1} or so, which were covered by O—H hydroxyl absorption band. Compared with CMCS (see curve b), a new shoulder absorption band assigned to the C=O stretch of ester group was observed at 1700 cm^{-1} in the spectrum of NBS–CMCS (see curve c). The characteristic bands at 1249 cm^{-1} and 1055 cm^{-1} were attributed to the C—O stretch of ester group. Besides, the characteristic bands at 1654 and 1573 cm^{-1} observably increased after conjugation, which were attributed to the carbonyl of amide I band and N—H bending of amide II band, respectively. All the above results confirm the formation of amide linkage between the carboxyl group of NBS and the amino groups of CMCS.

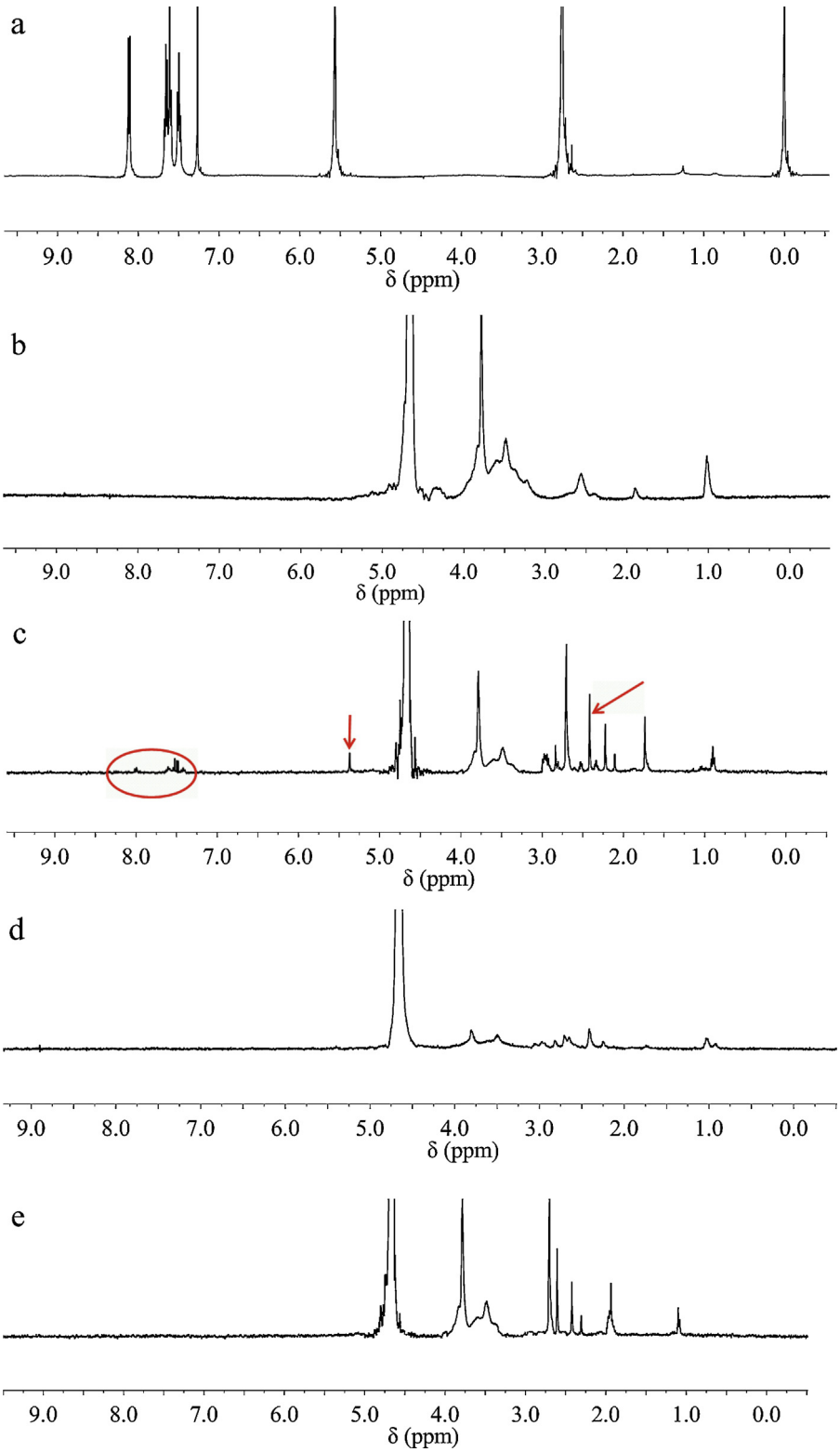

Fig. 2. ^{1}H NMR spectra of (a) NBS in $CDCl_3$, (b) CMCS in D_2O, (c) NBS–CMCS in DMSO–d_6/D_2O (1:3, v/v), (d) NBS–CMCS in D_2O, and (e) photolytic product in DMSO–d_6/D_2O (1:3, v/v) after UV radiation.

3.2. Formation and characterization of micelles

Amphiphilic polymer with a proper hydrophilic/hydrophobic balance can self-assemble into micelle structure in aqueous media. NBS–CMCS might self-assemble into core–shell micelles because of its amphiphilic structure comprised of hydrophobic NBS moieties and hydrophilic CMCS backbone. A procedure shown in Fig. 1(D) provides a description of NBS–CMCS micelle formation. Nile red was used as a fluorescence probe to monitor the process. If the polymeric micelles can form in an aqueous solution, Nile red molecules preferably locate inside the hydrophobic microdomains of micelles rather than the aqueous phase, resulting in different

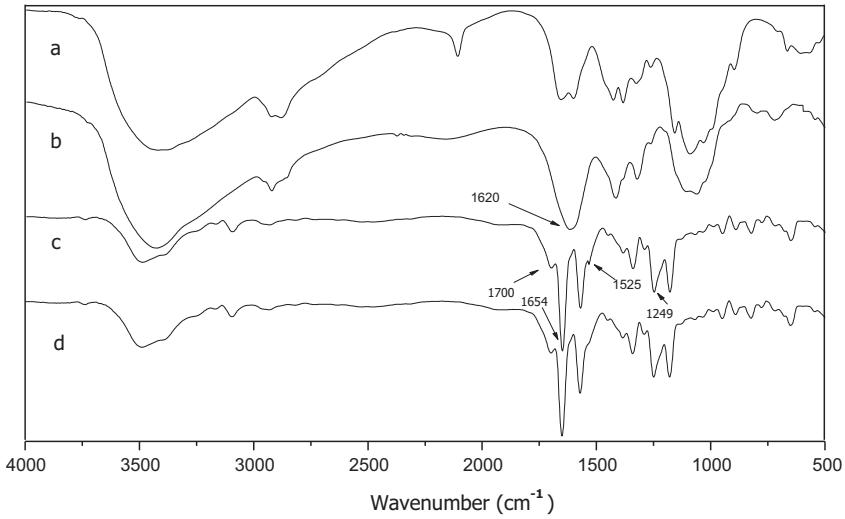

Fig. 3. FT-IR spectra of (a) CS, (b) CMCS, (c) NBS–CMCS, and (d) GA cross-linked NBS–CMCS.

photophysical characteristics. As shown in Fig. 5(A), with increase of NBS–CMCS concentration, the fluorescence emission intensity of Nile red increased very slowly in low concentration ranges. However, it increased dramatically at a certain concentration, implying the formation of micelles and encapsulation of Nile red into the hydrophobic cores (Kabanov & Alakov, 2002). This concentration can be defined as a critical micelle concentration (CMC). It is suggested in Fig. 5(A) that the CMC of NBS–CMCS-1 in water was about 0.057 mg/mL; while those of NBS–CMCS-2 and NBS–CMCS-3 determined by the same method decreased to 0.026 mg/mL and 0.019 mg/mL, respectively; this is obviously attributed to the enhanced hydrophobicity by increase of DS.

The evidence for the formation of the micelles was provided by TEM experiments. The image (a) in Fig. 4 reveals that there was obvious contrast between the peripheries and centers in the spheres, characteristic of the projection images of core–shell micelles.

The self-assembly behavior of NBS–CMCS was also investigated by means of ^{1}H NMR. The curve d in Fig. 2 shows ^{1}H NMR spectrum of lyophilized NBS–CMCS in D_2O. Compared with that of NBS–CMCS in DMSO–d_6/D_2O (see curve c), some signals at 2.46, 5.4, and 7.4–8.0 ppm ascribed to the protons of appended NBS groups, especially those signals at 7.4–8.0 ppm assignable to the aromatic protons, were not observed. It indicated that the hydrophobic NBS groups in NBS–CMCS was confined within the hydrophobic domains shielded by hydrophilic CMCS chain segments because of the formation of shelf-aggregates in D_2O, thus leading to proton signal shielding of NBS. The similar results were also observed for other amphiphilic polymers that forms micelles in the aqueous phase (Wang et al., 2011).

3.3. Characterization of shell cross-linked micelles

In pesticide delivery, an important issue need to be considered is the micelle structural integrity and pesticide encapsulation stability. When the polymer concentration falls below the critical micellization concentration (CMC) because of high dilution, polymeric micelles will dissociate accompanied with undesirable release of encapsulated pesticides before reaching the targeted sites (Nakamura, Ryuichi, & Takeda, 1976; Dubey, Jhelum, & Patanjali, 2011; Jiang, Liu, & Narain, 2009). Moreover, the physical encapsulation of pesticides within polymeric micelles will lead to premature pesticide release during storage and reduce the effectiveness of pesticides. To enhance the micellar structural integrity and drug encapsulation stability, we selected GA to cross-link the shell of NBS–CMCS micelles because GA can easily react with amino groups of NBS–CMCS (Fig. 1D). The FT-IR spectra of NBS–CMCS and GA cross-linked NBS–CMCS are exhibited in Fig. 3. An absorption band corresponding to the N—H bending at 1525 cm^{-1} of chains (see curve d) became very weak in the spectrum of GA cross-linked micelles. The observation indicates that cross-linking took place between the amine groups on NBS–CMCS chain and GA. The similar absorption band has also been observed in the literature (Wang et al., 2014).

To verify the GA cross-linking further, the concentrations of micelles were diluted to below CMC. It was found in our experiment that the uncross-linked micelles were dissociated. However, for cross-linked micelles, the particles nearly maintained the same size and PDI value upon high dilution, indicating a successful GA cross-linking and the ability of cross-linking to stabilize the micelles.

TEM measurements were also taken to evaluate the size and morphology of GA cross-linked micelles. As shown in Fig. 4(c), the morphology of cross-linked micelles is similar to that of uncross-linked micelles (see image a), while the average size decreases from 165 ± 6.3 nm to 140 ± 5.5 nm after cross-linking, showing the formation of more compact structures.

The size and distribution of GA cross-linked micelles were also measured by DLS (see Table 1). The diameters of cross-linked samples were smaller than those of uncross-linked. This result is consistent with that obtained by TEM observation. In addition to the cross-linking, the hydrophobic interaction also shows the influence on the nanoparticle size. The diameter of uncross-linked samples decreased slightly with increasing of DS of NBS, this is obviously ascribed to that the NBS–CMCS chain with the higher DS of NBS tends to coil a more shrinking structure. By contrast, a more significant effect of DS of NBS on the diameter of cross-linked samples was observed; showing that not only the hydrophobic interaction but also the cross-linking contributed to this result.

The zeta potential was a useful tool to predict the physical storage stability of colloidal particles. In our study, the zeta potential values of all samples were between -25.5 ± 1.24 mV and -30.5 ± 1.11 mV, which are near the critical value of -30 mV, indicating that all the micelles have good stability. To further confirm the prediction, GA cross-linked samples were stored for one month in the dark in the buffer of pH 7.0, their mean diameters and polydispersity index (PDI) values did not change significantly (as shown

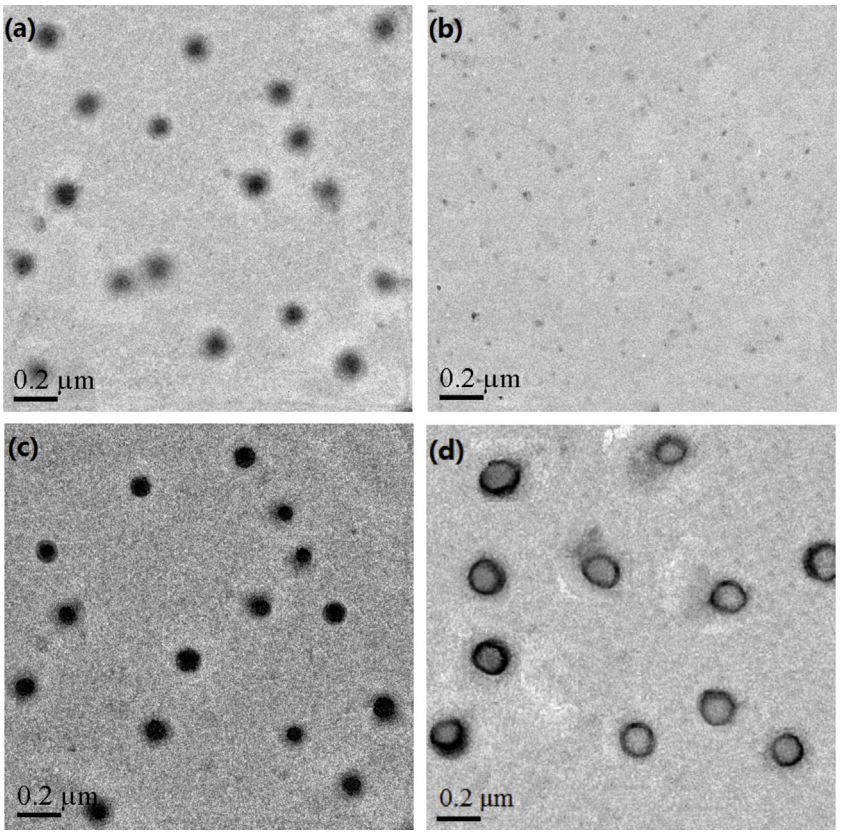

Fig. 4. Electron transmission microphotographs of (a) uncross-linked micelles before and (b) after UV irradiation as well as (c) cross-linked micelles before and (d) after UV irradiation.

in Table 1), whereas the those of the uncross-linked micelles had an increase to some extent, suggesting that the cross-linking micelles have higher stability.

3.4. Photo-responsive property of the shell cross-linked micelles

The photo-responsive properties of the shell cross-linked micelles were studied through DLS and TEM. As shown in Table 1, the average diameters of all micelle samples measured by DLS were between $196 \pm 0.11 \sim 242 \pm 0.04$ nm at pH 7.0. When the uncross-linked NBS–CMCS-2 micelle solution was irradiated under UV light for 10 min, the diameter measured by DLS decreased to about 40.6 nm (see Table 1). This implies that photoremovable side NBS groups were cleaved from CMCS main chains under UV irradiation, causing a formation of single molecule aggregate (Liu, Chen, Liu, & Liu, 2008; Chen, Du, Tian, & Sun, 2005). In contrast, the cross-linked NBS–CMCS-2 micelles allowed for the formation of a stable structure after photolysis, their average diameter increased from 196 ± 0.11 nm to 238 ± 0.20 nm. The increase in hydrodynamic diameter (Dh) after the removal of the hydrophobic core can be explained by the cross-linked CMCS shell acting like a hydrogel material and undergoing expansion as the core domain fills with water.

In order to further confirm the above speculation, the photo-response of shell cross-linked micelles was also investigated by TEM. As expected, the uncross-linked micelles disintegrated upon UV photolysis due to lack of covalent cross-linking (see image b in Fig. 4); while the shell cross-linked micelles resulted in a stable nanocapsule structure after UV irradiation (see image d in Fig. 4). Their average diameter increased from 140 ± 5.5 nm to 175 ± 6.8 nm. This result is consistent with that obtained by DLS.

The photo-response of NBS–CMCS micelles may be attributed to photolysis reaction of NBS–CMCS. Fig. 5(B) shows the UV absorption of the aqueous solution of NBS–CMCS-2 exposed to 365 nm radiation for different time. The characteristic peak of NBS at 260 nm decreased with increase of the irradiation time and leveled off after 8 min, indicating that the photolysis reaction took place under UV stimuli. The ^{1}H NMR from photolytic product in Fig. 2 (see curve e) further supports this result. The signals at 5.4 and 7.4–8.0 ppm ascribed to the protons of 2-nitrobenzyl in NBS were not observed in curve e, indicating that the phototriggers had been broken away from NBS–CMCS.

Table 2
The drug loading efficiency (LE) and encapsulation efficiency (EE) of diuron-loaded uncross-linked micelles and cross-linked micelles based on NBS–CMCS.

Conjugates	Feed ratio[a]	Uncross-linked micelles		Cross-linked micelles	
		EE (%)	LE (%)	EE (%)	LE (%)
NBS–CMCS-1	0.07	90.5	15.6	86.7	18.8
NBS–CMCS-2	0.15	95.6	37.6	91.9	40.2
NBS–CMCS-3	0.26	92.3	32.3	90.5	37.5

[a]Molar ratio of NBS to glucosamine units of CMCS.

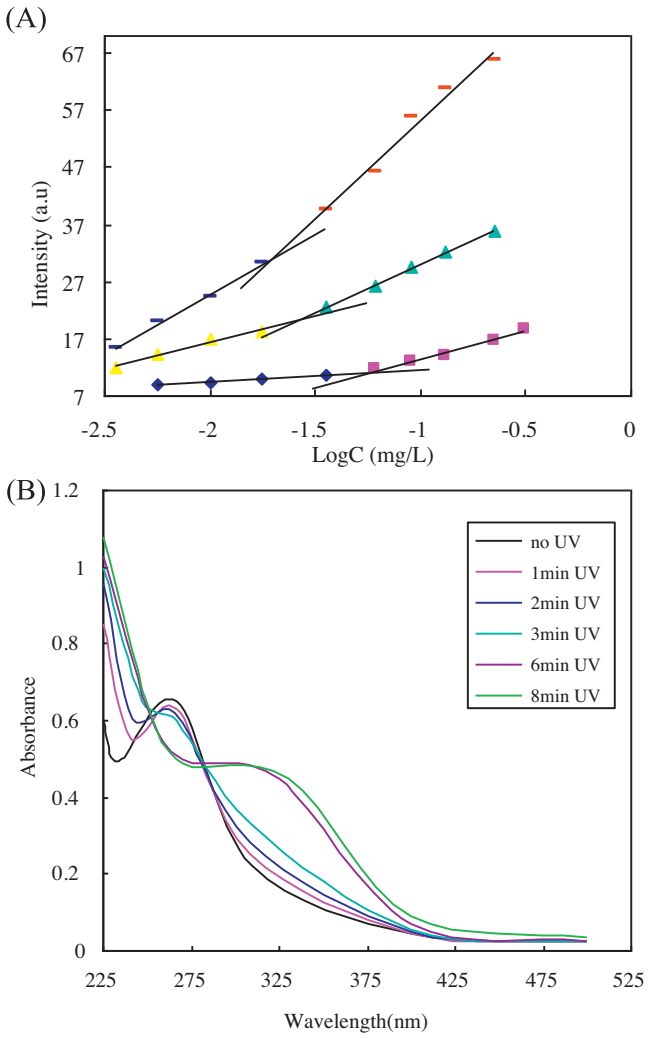

Fig. 5. (A) Emission intensity of Nile red as a function of the concentrations of (♦) NBS–CMCS-1, (▲) NBS–CMCS-2 and (—) NBS–CMCS-3. (B) UV–vis spectrum of NBS–CMCS-2 micelle aqueous solution exposed to 365 nm radiation for different time.

3.5. Diuron-loading of the shell cross-linked micelles

Core–shell polymeric micelles are particularly suitable for the encapsulation of hydrophobic active substances because of the hydrophobic interaction between the substances and the micelle core (Torchilin, 2004). Diuron is a hydrophobic herbicide, which is readily encapsulated into micelles in the process of assembly by mixing with NBS–CMCS solution. Table 2 lists the LE and EE of diuron-loaded uncross-linked micelles and cross-linked micelles. The encapsulation efficiency of cross-linked micelles based on NBS–CMCS-2 reached 91.9%, and the diuron loading efficiency reached 40.2%, indicating that diuron was efficiently encapsulated into the micelles. In addition, The LE of uncross-linked micelles was smaller than that of cross-linked micelles. This may be attributed to the GA cross-linking, which reduces the leakage of diuron.

3.6. Release studies of the diuron-loaded shell cross-linked micelles

In order to evaluate the potential of the photo-responsive NBS–CMCS micelles as a controlled release carrier of herbicide, the release behavior of the diuron encapsulated in NBS–CMCS micelles in pH 7.0 aqueous solution was studied. As presented in Fig. 6, without UV irradiation, the diuron release from the diuron-loaded shell cross-linked micelles was not detected, and only 3.35% of the loaded diuron was released within 8 h for the uncross-linked micelles. However, with UV irradiation, approximately 45.5% of the loaded diuron was released from the cross-linked sample within 2 min (see inset). With the further extension of exposure time to UV light, the diuron release increased and the cumulative amount was up to 96.9% at 10 min. These results indicate that the shell cross-linked micelles are able to release the encapsulated diuron in response to stimuli of UV light.

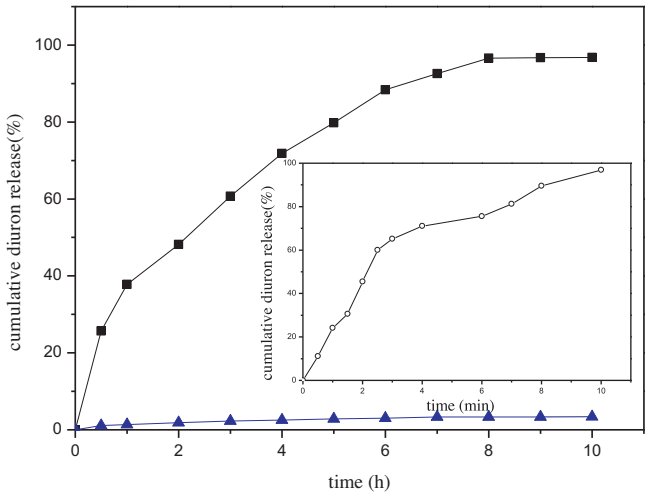

Fig. 6. Release of diuron from the diuron-loaded micelles based on NBS–CMCS-2 in a pH 7.0 buffer under different conditions of light exposure. (▲): uncross-linked micelles without light irradiation; (○): shell cross-linked micelles with UV (365 nm, 150 mW cm^{-2}) irradiation (see inset); (■): shell cross-linked micelles with solar simulated irradiation (200–2500 nm spectral output, 50 W radiant output).

Sunlight absorption of 2-nitrobenzyl-based chromophores has already been used to make photo-induced uncaging of bioactive substances (Sagar, Primavesi, Paul, & Davis, 2014). In order to find out whether the cross-linked NBS–CMCS micelles can also release the loaded diuron in response to sunlight, a 300 W Xenon arc lamp (200–2500 nm spectral output, 50 W radiant output) was used as solar-simulating radiation for evaluation of the response of the diuron-loaded cross-linked micelles. A gradual increase in release rate was observed over 8 h of irradiation (Fig. 6). This result indicates that the broadband can trigger a slow release of diuron from the cross-linked NBS–CMCS micelles.

4. Conclusions

In our study, a novel amphiphilic conjugate composed of hydrophilic carboxymethyl chitosan and hydrophobic photolabile 2-nitrobenzyl groups was synthesized and its structure was characterized by FT-IR and ^{1}HNMR. In deionized water the conjugate could self-assemble into polymeric micelles through the hydrophobic interactions between photolabile groups, and further form cross-linked photoresponsive micelles by dropwise adding of GA. TEM photograph and ^{1}H NMR investigation showed that the uncross-linked and cross-linked micelles had a spherical core–shell structure, which is especially suitable for the encapsulation of hydrophobic diruon.

Research by light scattering showed that the GA cross-linked micelles in the dark exhibited a high stability and a narrow size distribution, while an obvious increase in the average diameter was observed upon exposure to 365 nm UV. An observation by TEM showed that UV irradiation could trigger the transformation of the cross-linked micelles into a nanocage struture. The release from diuron-loaded cross-linked micelles was not detected over

8 h without light exposure, while a slow release could be observed under solar simulated irradiation, suggesting that the cross-linked micelles may be useful in the delivery of photosynthetic inhibitors to the sites of photosynthesis, and their further investigations are in progress.

Acknowledgments

This research was supported by National Natural Science Foundation of China (No. 51373130) and the Natural Science Foundation for the Youth (No. 51303145).

References

Brugnerotto, J., Lizardi, J., Goycoolea, F. M., Arguelles-Monal, W., Desbrieres, J., & Rinaudo, M. (2001). An infrared investigation in relation with chitin and chitosan characterization. *Polymer*, *42*, 3569–3580.

Chen, L., Du, Y., Tian, Z., & Sun, L. (2005). Effect of the degree of deacetylation and the substitution of carboxymethyl chitosan on its aggregation behavior. *Journal of Polymer Science Part B: Polymer Physics*, *43*, 296–305.

Chen, X.-G., & Park, J. (2003). Chemical characteristics of *O*-carboxymethyl chitosans related to the preparation conditions. *Carbohydrate Polymers*, *53*, 355–359.

Dubey, S., Jhelum, V., & Patanjali, P. K. (2011). Controlled release agrochemicals formulations: A review. *Journal of Scientific & Industrial Research*, *70*, 105–112.

Feng, C., Wang, Z., Jiang, C., Kong, M., Zhou, X., Li, Y., et al. (2013). Chitosan/*O*-carboxymethyl chitosan nanoparticles for efficient and safe oral anticancer drug delivery: In vitro and in vivo evaluation. *International Journal of Pharmaceutics*, *457*, 158–167.

He, J., Tong, X., & Zhao, Y. (2009). Photoresponsive naogels based on photocontrollable cross-links. *Marcromolecules*, *42*, 4845–4852.

Hjerde, R. J. N., Varum, K. M., Grasdalen, H., Tokura, S., & Smidsrod, O. (1997). Chemical composition of *O*-(carboxymethyl)-chitins in relation to lysozyme degradation rates. *Carbohydrate Polymers*, *34*, 131–139.

Jiang, J., Qi, B., Lepage, M., & Zhao, Y. (2007). Polymer micelles stabilization on demand through photo-cross-linking. *Marcromolecules*, *40*, 790–792.

Jiang, J., Tong, X., Morris, D., & Zhao, Y. (2006). Toward photocontrolled realease using light-dissociate block copolymer micelles. *Macromolecules*, *39*, 4633–4640.

Jiang, X., Liu, S., & Narain, R. (2009). Degradable thermoresponsive core cross-linked micelles: Fabrication, surface functionalization, and biorecongnition. *Langmuir*, *25*, 13344–13350.

Kabanov, A. V., & Alakov, V. Y. (2002). Pluronic block copolymers in drug delivery: From micellar nanocontainers to biological response modifiers. *Critical Reviews in Therapeutic Drug Carrier Systems*, *19*, 1–72.

Kindermann, M., George, N., Johnsson, N., & Johnsson, K. (2003). Covalent and selective immobilization of fusion proteins. *Journal of the American Chemical Society*, *125*, 7810–7811.

Li, N., Li, X., Zhou, Y., Li, W., Zhao, Y., & Ma, S. (2012). The use of polyion complex micelles to enhance the oral delivery of salmon calcitonin and transport mechanism across the intestinal epithelial barrier. *Biomaterials*, *33*, 8881–8892.

Liu, K.-H., Chen, S.-Y., Liu, D.-M., & Liu, D.-M. (2008). Self-assembled hollow nanocapsule from amphiphatic carboxymethyl-hexanoyl chitosan as drug carrier. *Macromolecules*, *41*, 6511–6516.

Luo, Y., Teng, Z., Wang, X., & Wang, Q. (2013). Development of carboxymethyl chitosan hydrogel beads in alcohol-aqueous binary solvent for nutrient delivery applications. *Food Hydrocolloids*, *31*, 332–339.

Margni, M., Rossier, D., Crettaz, P., & Jolliet, O. (2002). Life cycle impact assessment of pesticides on human health and ecosystems. *Agriculture, Ecosystems & Environment*, *93*, 379–392.

Mathot, F., van Beijsterveldt, L., Preat, V., Brewster, M., & Arien, A. (2006). Intestinal uptake and biodistribution of novel polymeric micelles after oral administration. *Journal of Controlled Release*, *111*, 47–55.

Meng, L., Huang, W., Wang, D., Huang, X., Zhu, X., & Yan, D. (2013). Chitosan-based nanocarriers with pH and light dual response for anticancer drug delivery. *Biomacromolecules*, *14*, 2601–2610.

Muzzarelli, R. A. A., Tanfani, F., Emanuel, M., & Mariotti, S. (1982). *N*-(carboxymethylidene) chitosans and *N*-(carboxymethyl) chitosans: Novel chelating polyampholytes obtained from chitosan glyoxylate. *Carbohydrate Research*, *107*, 199–214.

Nakamura, K., Ryuichi, E., & Takeda, M. (1976). Surface properties of styrene–ethylene oxide block copolymers. *Journal of Polymer Science*, *14*, 1287–1295.

Sagar, R., Primavesi, L.F., Paul, M., & Davis, B.G., 2014. Modification of trehalose-6-phosphate levels in plants. WO 2012/146914 A1, 22–27.

Sopeña, F., Maqueda, C., & Morillo, E. (2009). Controlled release formulations of herbicides based on micro-encapsulation. *Ciencia e Investigación Agraria*, *36*, 27–42.

Sun, C., Shu, K., Wang, W., Ye, Z., Liu, T., Gao, Y., et al. (2014). Encapsulation and controlled release of hydrophilic pesticide in shell cross-linked nanocapsules containing aqueous core. *International Journal of Pharmaceutics*, *463*, 108–114.

Tasmin, R., Shimasaki, Y., Tsuyama, M., Qiu, X., Khalil, F., Okino, N., et al. (2014). Elevated water temperature reduces the acute toxicity of the widely used herbicide diuron to a green alga, *Pseudokirchneriella subcapitata*. *Environmental Science and Pollution Research*, *21*, 1064–1070.

Torchilin, V. P. (2004). Targeted polymeric micelles for delivery of poorly soluble drugs. *Cellular & Molecular Life Sciences Cmls*, *61*(19–20), 2549–2559.

Wang, F., Zhang, D., Duan, C., Jia, L., Feng, F., Liu, Y., et al. (2011). Preparation and characterization of a novel deoxycholic acid-*O*-carboxymethylated chitosan-folic acid conjugates and self-aggregates. *Carbohydrate Polymers*, *84*, 1192–1200.

Wang, X., Dahamni, F. Z., Chen, Y., Yin, L., Zhou, J., & Yao, J. (2014). Amphiphilic carboxymethyl chitosan-quercetin conjugate with P-gp inhibitory properties for oral delivery of paclitaxel. *Biomaterials, 35*, 7654–7665.

Wang, Y., Ma, N., Wang, Z., & Zhang, X. (2007). Photocontrolled reversible supramolecule assemblies of an azobenzene-containing surfactant with a-cyclodextrin. *Angewandte Chemie International Edition*, *46*, 2823–2826.

Yamamoto, H., & Nakamura, K. (2003). Sampling sediment and water in rice paddy fields and adjacent water bodies. In P. W. Lee, H. Aizawa, A. C. Barefoot, & J. J. Murphy (Eds.), *Handbook of residue analytical methods for agrochemicals* (vols. 1 & 2) (pp. 892–907). Chichester, West Sussex, England/Hoboken, NJ, USA: Wiley. ISBN: 0-4714-9194-2.

Yan, F., Chen, L., Tang, Q., & Wang, R. (2004). Syhthesis and characterization of a photocleavable cross-linker and its application on tunable surface modification and pritein photodelivery. *Bioconjugate Chemistry*, *15*, 1030–1036.

Yin, Y., Lv, X., Tu, H., Xu, S., & Zheng, H. (2010). Preparation and swelling kinetics of pH- sensitive photocrosslinked hydrogel based on carboxymethyl chitosan. *Journal of Polymer Research*, *17*, 471–479.

Yi, Y., Xu, S., Sun, H., Chang, D., Yin, Y., Zheng, H., et al. (2011). Gelation of photocrosslinkable carboxymethyl chitosan and its application in controlled release of pesticide. *Carbohydrate Polymers*, *86*, 1007–1013.